Available online at www.sciencedirect.com
ScienceDirect
Journal of the European Ceramic Society 31 (2011) 1309–1316
www.elsevier.com/locate/jeurceramsoc

Microstructural and mechanical evaluation of a Cu-based active braze alloy to join silicon nitride ceramics

M. Singh [a,*], Rajiv Asthana [b], F.M. Varela [c], J. Martínez-Fernández [c]

[a] Ohio Aerospace Institute, NASA Glenn Research Center, Cleveland, OH 44135, USA
[b] Department of Engineering and Technology, University of Wisconsin-Stout, Menomonie, WI 54751, USA
[c] Dpto. Física de la Materia Condensada-ICMSE, Universidad de Sevilla-CSIC, Avda. Reina Mercedes, s/n, 41012 Sevilla, Spain

Available online 6 August 2010

Abstract

Self-joining of St. Gobain Si_3N_4 (NT-154) using a ductile Cu–Al–Si–Ti active braze (Cu-ABA) was demonstrated. A reaction zone (~2.5–3.5 μm thick) developed at the interface after 30 min brazing at 1317 K. The interface was enriched in Ti and Si. The room temperature compressive shear strengths of Si_3N_4/Si_3N_4 and Inconel/Inconel joints (the latter created to access baseline data for use with the proposed Si_3N_4/Inconel joints) were 140 ± 49 MPa and 207 ± 12 MPa, respectively. High-temperature shear tests were performed at 1023 K and 1073 K, and the strength of the Si_3N_4/Si_3N_4 and Inconel/Inconel joints were determined. The joints were metallurgically well-bonded for temperatures above 2/3 of the braze solidus. Scanning and transmission electron microscopy studies revealed a fine grain microstructure in the reaction layer, and large grains in the inner part of the joint with interfaces being crack-free. The observed formation of Ti_5Si_3 and AlN at the joint interface during brazing is discussed.

Keywords: Silicon nitride; Brazing; Joints; High-temperature strength; Microstructure

1. Introduction

Silicon nitride (Si_3N_4) is a light-weight ceramic with excellent high-temperature strength, creep-resistance, low thermal expansion, and excellent resistance to thermal shock, wear, and oxidation. This material is currently used in reciprocating engine components, turbochargers, auxiliary power unit components for aircraft, bearings, and metal cutting tools. There is increasing interest in Si_3N_4 for use in turbine components of the next-generation turbo-shaft engines because of its potential to be deployed without the need for extensive cooling as required when using metallic parts. Their use projected to significantly raise engine efficiency and performance.

Si_3N_4 is particularly suitable for small turbine engine components which may be easier to fabricate than SiC/SiC fiber composites because of the inherent complexity in weaving cooling channels and sharp edges using the SiC fibers. However, in a number of applications, relatively complex geometrical designs of Si_3N_4 parts are needed. As shaping of Si_3N_4 is less amenable to machining and conventional manufacturing, robust and affordable joining techniques that are capable of integrating geometrically simpler Si_3N_4 parts into complex components play a critical enabling role. Thus, one key aspect of Si_3N_4 utilization in emerging applications is its joining response to diverse materials. In an ongoing research program, the joining and integration of Si_3N_4 ceramics with metallic, ceramic, and composite materials using braze interlayers with the liquidus temperature in the range 1023–1513 K is being investigated.

Among the filler metals used to join Si_3N_4 ceramics, Ag–Cu eutectic alloys containing Ti have been the most widely used.[1–4] Other notable fillers include Ag–Cu–In and Ag–Cu–Sn containing Ti. Besides Ti, active elements such as Hf, Zr, Nb and Ta also have been evaluated for joining Si_3N_4. In addition, active brazes such as Pd–Ni–Ti, Au–Pd–Ti, and Cu–Pt–Ti/Nb as well as non-reactive brazes Pd–Ni and Au–Pd–Ni in conjunction with premetallized Si_3N_4 also have been used. The active metal Cr has been used in Ni–Pd and Ni–Si eutectics.[5] Numerous other brazes have been used to join Si_3N_4 ceramics.[6–24] Nevertheless, the Ag–Cu–Ti fillers are known to produce the highest levels of joint integrity and are most extensively used with silicon nitride ceramics. There also is interest in evaluating brazes with melting points higher than the Ag–Cu–Ti fillers to join Si_3N_4.

* Corresponding author.
E-mail address: mrityunjay.singh-1@nasa.gov (M. Singh).

0955-2219/$ – see front matter © 2010 Elsevier Ltd. All rights reserved.
doi:10.1016/j.jeurceramsoc.2010.07.022

In this study, we utilize an active braze, Cu-ABA, that has a higher liquidus temperature ($T_L \sim 1297$ K) than Ag–Cu eutectic brazes containing Ti. The self-joining behavior of a widely available commercial variety of Si_3N_4 using Cu-ABA is investigated. In particular, joint microstructure, composition, and joint strength at room and elevated temperatures, as revealed by optical microscopy, scanning electron microscopy (SEM), energy dispersive spectroscopy (EDS), transmission electron microscopy (TEM), and offset compression shear test, are presented and discussed.

2. Experimental procedures

2.1. Joint fabrication

St. Gobain Si_3N_4 (NT-154) containing 4 wt.% Y_2O_3 as a sintering aid was used for joining. Studies have shown that thin nanometric intergranular amorphous films of yttrium silicate glasses form at grain boundaries in Si_3N_4 containing yttria.[25] The Si_3N_4 material was self-brazed using a commercial Cu–Si–Al–Ti braze alloy, Cu-ABA (from Morgan Advanced Ceramics, CA), with a nominal composition (in wt.%) of 92.75Cu–3Si–2Al–2.25Ti, and with the solidus and liquidus temperatures of $T_S \sim 1231$ K and $T_L \sim 1297$ K, respectively. The Cu-ABA braze has high ductility (42%) and was obtained in foil form (thickness ~50 μm). The elastic modulus, yield strength and tensile strength of Cu-ABA are 96 GPa, 278 MPa, and 520 MPa, respectively, and its coefficient of thermal expansion (CTE) is 19.5×10^{-6}/K.

The substrates and braze foils were sliced into 2.54 cm × 1.25 cm × 0.25 cm pieces, and ultrasonically cleaned in acetone for 15 min. Two braze foils were sandwiched between the substrates, and a load of ~1–2 N (~3.5–7.2 kPa pressure) was applied during brazing. The assembly was heated in a furnace to ~15–20 K above braze T_L under vacuum (~10^{-6} Torr), soaked for 30 min, and slowly cooled to room temperature.

2.2. Mechanical testing

The shear strength testing was done both at room temperature and two elevated temperatures (1023 K and 1073 K) under compressive loading on an Instron 8562 machine using hydraulic grip platens and a SS316 die for loading. For elevated temperature tests, a special hot stage was attached to the Instron unit. The temperatures of 1023 K and 1073 K represent rather severe test conditions, and are just 208 K and 158 K, respectively, below the braze solidus. A loading rate of 50 N/s was used and a deflectometer (Instron LVDT 2602-061) was used to record the displacement. Typically 3–5 specimens were tested for strength.

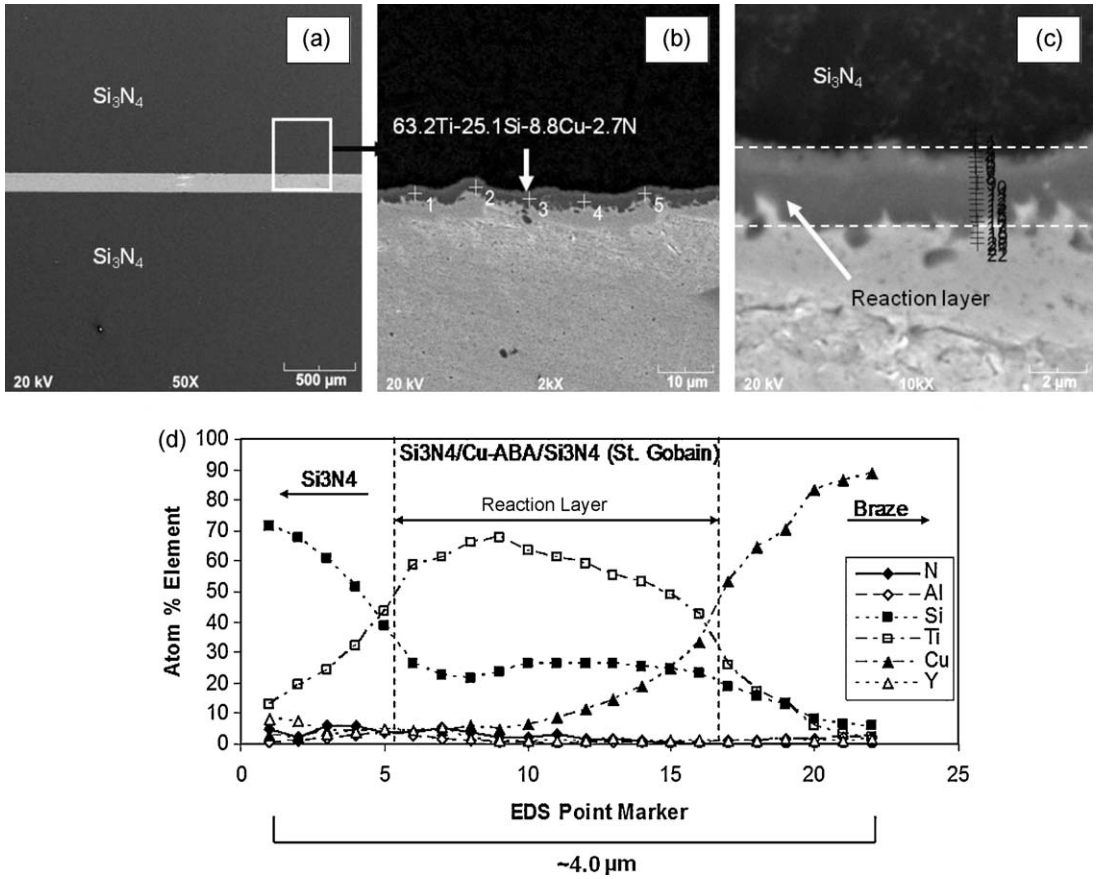

Fig. 1. (a–c) Joint microstructure and (d) elemental distribution in self-joined St. Gobain NT-154 Si_3N_4 material brazed at 1317 K for 30 min. The EDS data in (d) correspond to the point markers shown in (c).

Microhardness scans were made across the joint region with a Knoop micro-indenter on a Struers Duramin A-300 machine under a load of 200 g and loading time of 10 s.

2.3. Microstructural observations

The brazed joints were prepared for metallurgical examination and observed using SEM and EDS on a Philips XL30 electron microscope. Foils were prepared from the joints using conventional techniques and ion thinned to electron transparency. Microprobe EDS microanalyses were also performed on these foils. TEM observations were done using a Philips CM200 electron microscope.

3. Results and discussion

3.1. Microstructure

Fig. 1a displays a brazed silicon nitride joint made using the St. Gobain material (NT-154). Brazing with Cu-ABA for 30 min led to a homogenous, featureless (in the SEM observations) and compact reaction layer which is about 2.5–3.5 μm in thickness (Fig. 1b and c). This featureless product phase layer presumably formed from the coalescence of coarsened silicide crystals. It is conceivable that the product phase growth is initially controlled by the rate of the chemical reaction and later, when an appreciable thickness has developed, the growth kinetics are limited by the slower process of diffusion of reacting species across an already formed reaction layer.

Joint formation is promoted by the reactions which yield low contact angles of braze on Si_3N_4 substrates. In the case of Cu-ABA, pure Cu does not wet Si_3N_4 but Al wets Si_3N_4 under low pO_2 and high-temperatures because of disruption of oxide film on Al and formation of AlN or SiAlON compounds (Si in Cu-ABA improves the braze fluidity but probably does not affect the contact angle). Contact angle measurements[26–28] show that Ti-containing brazes rapidly wet the ceramic, and the most significant gains are achieved at small (2–10%) amounts of Ti at which braze ductility is not impaired but there is sufficiently high Ti activity for reactions with Si_3N_4. The metallurgically sound joints formed using Cu-ABA in this study attest to the role of Ti in improving the wetting and bonding of Si_3N_4.

The EDS analysis (Fig. 1d) of brazed Si_3N_4/Cu-ABA/Si_3N_4 joints shows that the layer is rich in Ti and Si. The X-ray spot analysis at several point markers along the reaction layer (Fig. 1b) revealed that the approximate average atomic concentration of this layer is 63Ti–25Si–9Cu–3N. This is qualitatively consistent with the literature studies according to which formation of complex Ti–Si–Cu–N compound layers is observed in silicon nitride joints brazed using Ag–Cu–Ti brazes.[2] There is no evidence of interfacial de-cohesion in the joint region.

EDS compositional maps were obtained during SEM (Fig. 2a and b) to determine the elemental spatial distribution. The compositional maps showed clearly that titanium was mainly

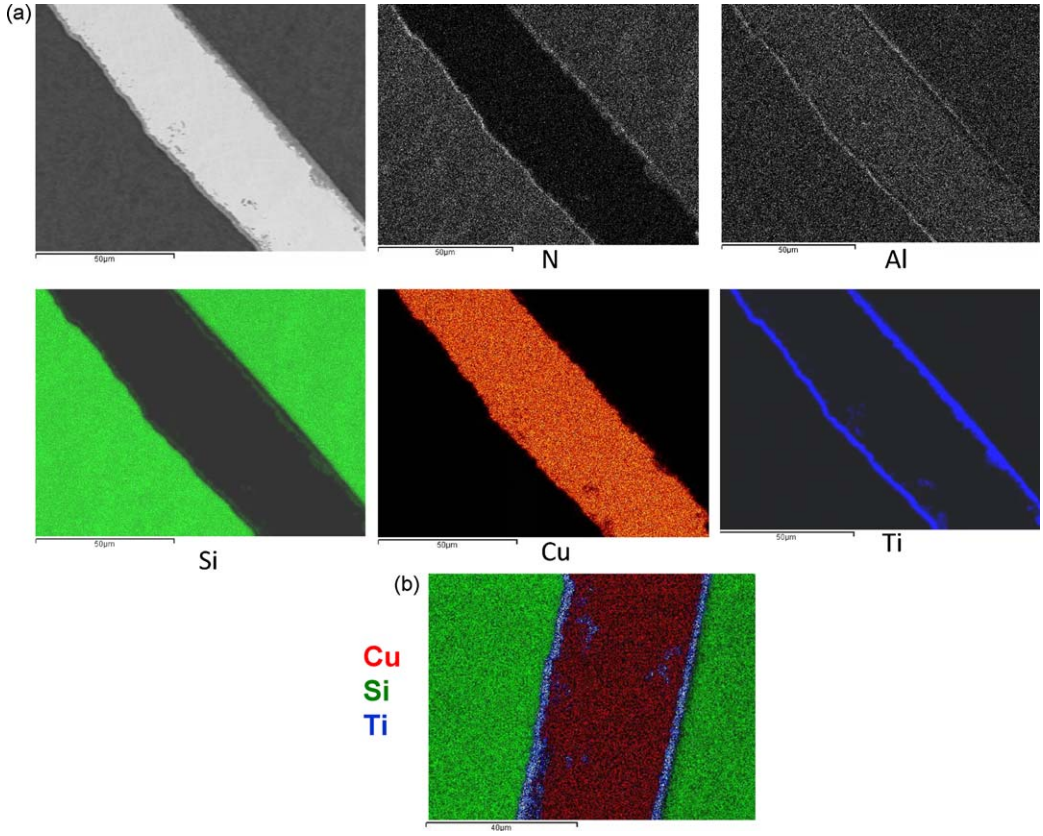

Fig. 2. (a) EDS compositional maps of the joint. Titanium segregation to the reaction layer can be easily visualized. Only small cluster Ti rich areas Ti remain in the joint interior. (b) Composition obtained superimposing the EDS compositional maps of the joint. (c) Lineal EDS profiles indicating the signal intensity corresponding to each element. (d) Composition obtained superimposing the line EDS profiles that shows the relative position of the compositional distributions.

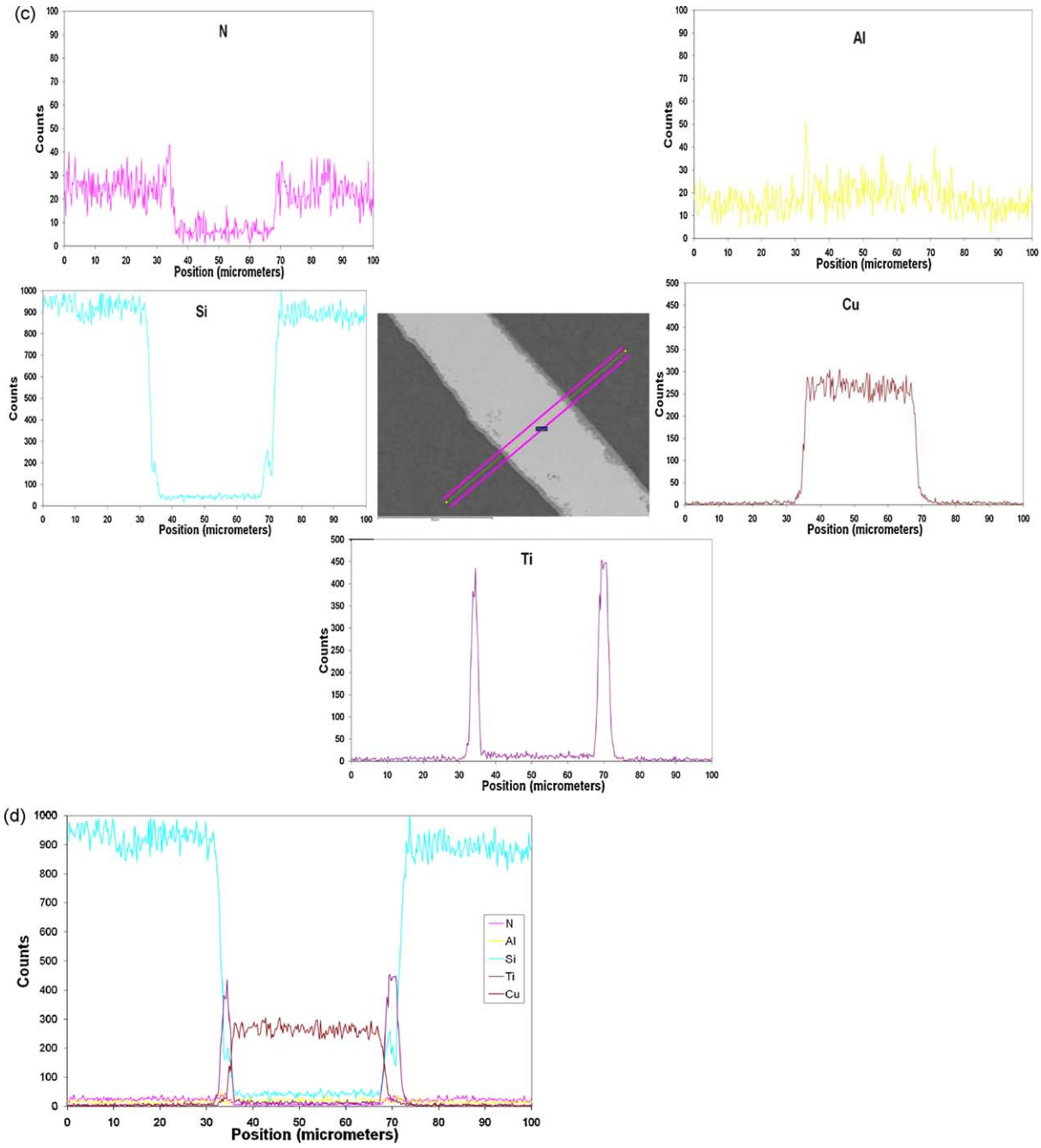

Fig. 2. (*Continued*).

deposited at the Cu-ABA/Si_3N_4 interface. Only small cluster areas containing Ti remain in the joint interior, whereas the copper was uniformly distributed along the joint region. It is interesting to note how the Ti-rich clusters are spatially coincident with Si rich clusters. The EDS compositional maps also show a fine bright contrast of the Al and N concentration at the Cu-ABA/Si_3N_4 interface, by far less evident than the Ti signal, but still noticeable.

The line EDS compositional lineal scan obtained during SEM observations (Fig. 2c), agrees with the previous observation and give additional spatial resolution. The high Ti concentration at the Cu-ABA/Si_3N_4 interface is clear, and some evidence of N and Al segregation at the Cu-ABA/Si_3N_4 interface can be inferred. Fig. 2d shows a composition scan obtained by superimposing the line EDS profiles that indicates the relative position of the compositional distributions.

TEM observations showed that the Si_3N_4 had a morphology consisting of large grains (micron size), but the reaction layer microstructure (Fig. 3a) had finer grains (in the range of 20–50 nm, Fig. 3b and c). The inner part of the joint was thinned rapidly during sample preparation, and it had a grain size intermediate between the one of the silicon nitride and the reaction layer. The interfaces between these three regions did not show cracks or defects that could nucleate failure. It is interesting to note that the reaction layer thinned during ion milling at a slower rate than the metallic inner part of the joint and the Si_3N_4,

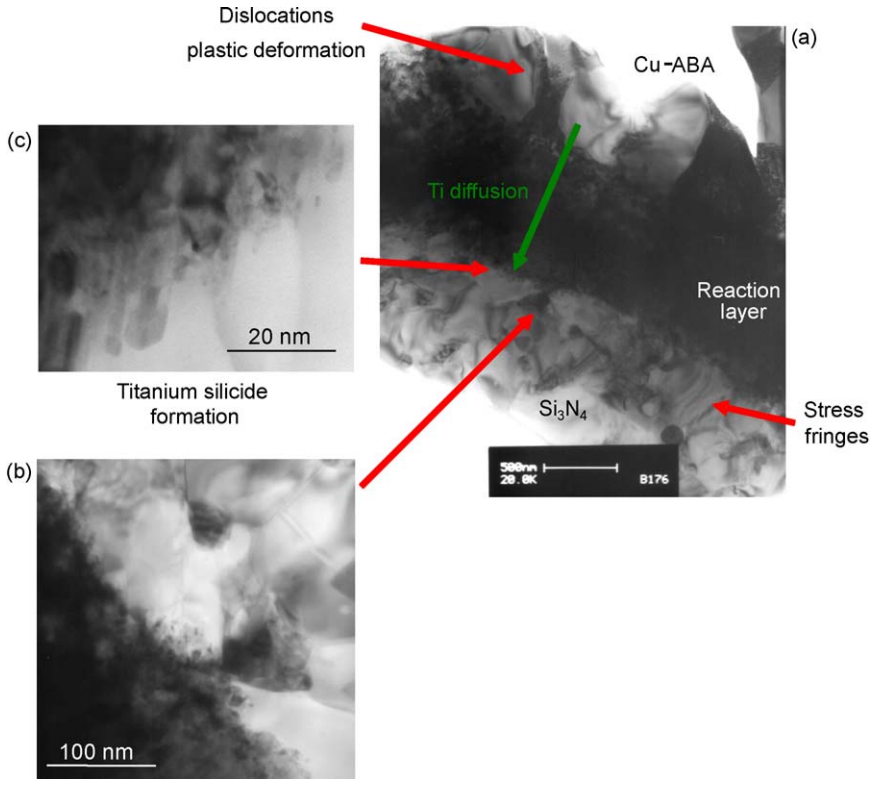

Fig. 3. TEM micrographs showing (a) the reaction layer at the Si_3N/braze interface and dislocations in braze, (b) titanium silicide formation, and (c) a higher magnification image of region shown in (b).

indicating the formation of new phases, most probably titanium silicides.

Fig. 3 includes higher magnification TEM micrographs (Fig. 3b and c) showing details of the reaction layer/Si_3N_4 interface in which evidence of the early stages of the titanium silicide formation (Fig. 3c) can be found. After an initial thickness of the reaction layer is formed, the process must be controlled by Ti diffusion through this reaction layer. The inner part of the joint (Cu-ABA) shows the presence of dislocations, indicating plastic deformation generated during brazing or subsequent testing. Si_3N_4 shows small strain fringes indicating stresses associated with elastic deformation to accommodate strain. However the mismatch strain, associated with the different dilatation coefficients, is not significant and does not create any damage in the joint area.

Fig. 4 shows electron diffraction patterns in the vicinity of the reaction layer/Si_3N_4 interface. The Si_3N_4 and Cu structure is in agreement with the diffraction pattern. Fig. 4b also includes an electron diffraction pattern in the reaction layer. These diffraction patterns are difficult to obtain due to the higher thickness of the foil in this region after ion thinning. The combination of higher thickness and nanometric grain size results in complex diffraction patterns.

EDS measurements were taken with a microprobe in the TEM mode to obtain analytical higher resolution (Fig. 5). The detail of these measurements in the Si_3N_4–reaction layer interface, gives additional information on concentration distribution of the phases present. There is an increase in the Al concentration at this interface in a region of less than 500 nm width. This thin region

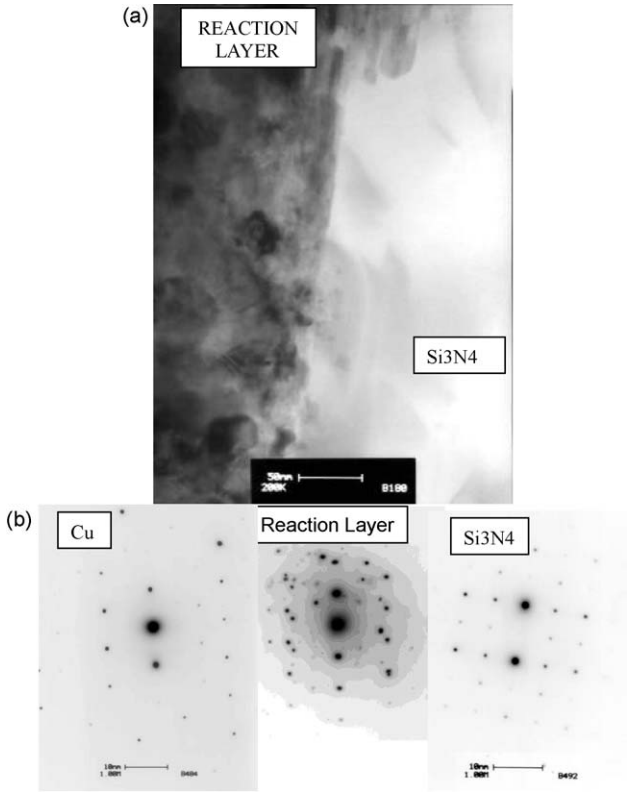

Fig. 4. (a) TEM micrographs showing the joint microstructure. Fine grains (<50 nm) form the reaction layer. (b) Electron diffraction patterns of the Si_3N_4, reaction layer and joint interior (Cu-ABA).

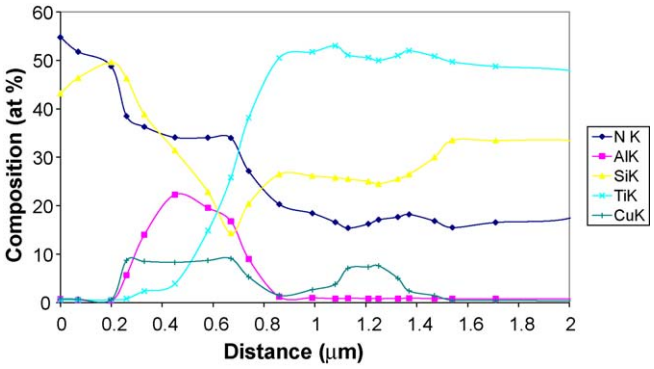

Fig. 5. Microprobe EDS analysis on TEM, that shows in more detail the compositional distribution in the vicinity of the interface Si_3N_4-reaction layer.

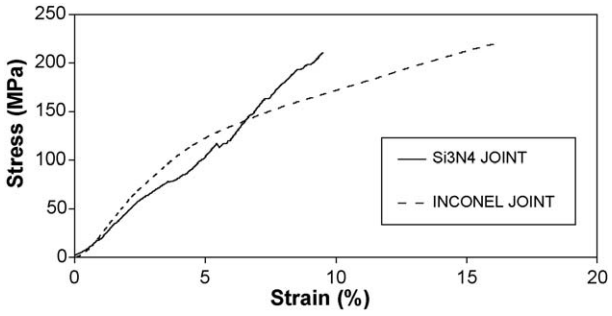

Fig. 6. Stress–strain plots from compression shear stress test at room temperature on brazed Si_3N_4/Cu-ABA/Si_3N_4 (NT-154) joints, and Inconel/Cu-ABA/Inconel joints.

has lower Ti and Si concentrations, and higher N concentration than the rest of the reaction layer, supporting the possibility of AlN formation. This is consistent with the thermodynamic calculations discussed below.

Reactions between Ti (in Cu-ABA) and Si_3N_4 could form titanium nitride (TiN) and titanium silicide (Ti_5Si_3) during brazing. Al in the Cu-ABA could also react and form AlN. Possible chemical reactions and the corresponding free energy changes (per mole of Ti or Al) at 1317 K (1044 °C), calculated using the software HSC Chemistry version 4.1 (Outokumpu Ra, Oy, Finland), are:

$$1/4Si_3N_4 + Ti = TiN + 3/4Si, \quad \Delta G_{1317\,K} = -136.46\,kJ \tag{1}$$

$$1/5Si_3N_4 + Ti = 1/5Ti_5Si_3 + 2/5\,N_2 \quad \Delta G_{1317\,K} = -56.19\,kJ \tag{2}$$

$$1/4Si_3N_4 + Al = AlN + 3/4Si, \quad \Delta G_{1317\,K} = -97.36\,kJ \tag{3}$$

$$Ti + 2Si = TiSi_2, \quad \Delta G_{1317\,K} = -162.13\,kJ \tag{4}$$

$$1/9Si_3N_4 + Ti = 4/9TiN + 1/9Ti_5Si_3, \quad \Delta G_{1317\,K} = -126.15\,kJ \tag{5}$$

$$2/3Si_3N_4 + Ti = TiSi_2 + 4/3\,N_2, \quad \Delta G_{1317\,K} = +43.56\,kJ \tag{6}$$

$TiSi_2$ formation from reaction (6) is unlikely as $\Delta G_{1317K} > 0$. In addition, $TiSi_2$ formation from reaction (4) is also unlikely even though $\Delta G_{1317K} = -162.13$ kJ, because there is no free Si. On the contrary, Ti_5Si_3 formation is likely because the reactions (2) and (5) responsible for its formation both have $\Delta G < 0$ (particularly reaction (5) with $\Delta G_{1317K} = -126.15$ kJ). Regarding AlN formation, the reaction 1/4 Si_3N_4 + Al = AlN + 3/4 Si has $\Delta G_{1317K} = -97.36$ kJ, which shows the thermodynamic feasibility of AlN formation. These conclusions are consistent with the EDS/TEM observations.

The analysis described above indicates that the reaction layer must be rich in the Ti_5Si_3, which is in good agreement with the atomic composition ratio and thermodynamic calculations. These analyses also support the AlN formation at Si_3N_4–reaction layer interface. Additionally, complex Ti–Si–Cu–N compound layers could also form in Si_3N_4 joints brazed using Ag–Cu–Ti brazes.

3.2. Mechanical properties

A compressive shear stress versus strain plot for Si_3N_4/Cu-ABA/Si_3N_4 (St. Gobain) joints at room temperature is shown in Fig. 6. The plot does not reveal any non-linearity which suggests that the braze and Si_3N_4 presumably did not plastically deform during testing. The fracture stress obtained from multiple tests is in the range 103–211 MPa, with the mean and standard deviation values of 140 MPa and 49 MPa, respectively. Observations of tested Si_3N_4/Si_3N_4 joints showed that fracture had propagated through Si_3N_4, not in the joint region. A shear stress versus strain plot for Inconel/Cu-ABA/Inconel joint is also shown in Fig. 6. The fracture stress of the Inconel/Inconel joint, based on multiple tests, was in the range 190–220 MPa, with the mean and standard deviation of 207 MPa and 12 MPa, respectively.

High-temperature compressive shear tests (Fig. 7) yielded the strength values of the Si_3N_4/Si_3N_4 joints at 1023 K and 1073 K as 45 ± 10 MPa and 35 ± 5 MPa, respectively, and the strength of Inconel/Inconel joints at 1023 K and 1073 K as 110 ± 10 MPa and 78 ± 5 MPa, respectively. These initial test results are very promising as they suggest that even at 260 K above a temperature equal to the 2/3rd of braze solidus, the Si_3N_4/Si_3N_4 joints had a shear strength comparable in magnitude to the room temperature yield strength of pure Al (35 MPa). The temperatures of 1023 K and 1073 K represent rather severe test conditions because these temperatures are just 208 K and 158 K, respectively, below the braze solidus temperature.

Knoop microhardness data are shown in Fig. 8. Fig. 8a shows indentations performed at the same load (200 g) in the joint and the Si_3N_4 sample. In Fig. 8b the Knoop hardness is plot-

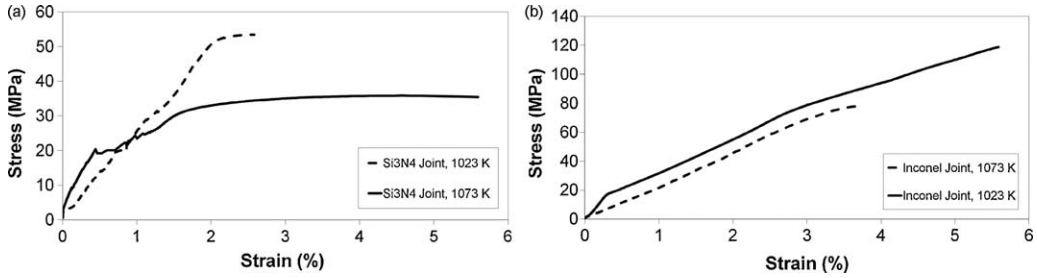

Fig. 7. Stress–strain plots from compression shear stress test at 1023 K and 1073 K on brazed (a) Si_3N_4/Cu-ABA/Si_3N_4 (NT-154) joints, and (b) Inconel/Cu-ABA/Inconel joints.

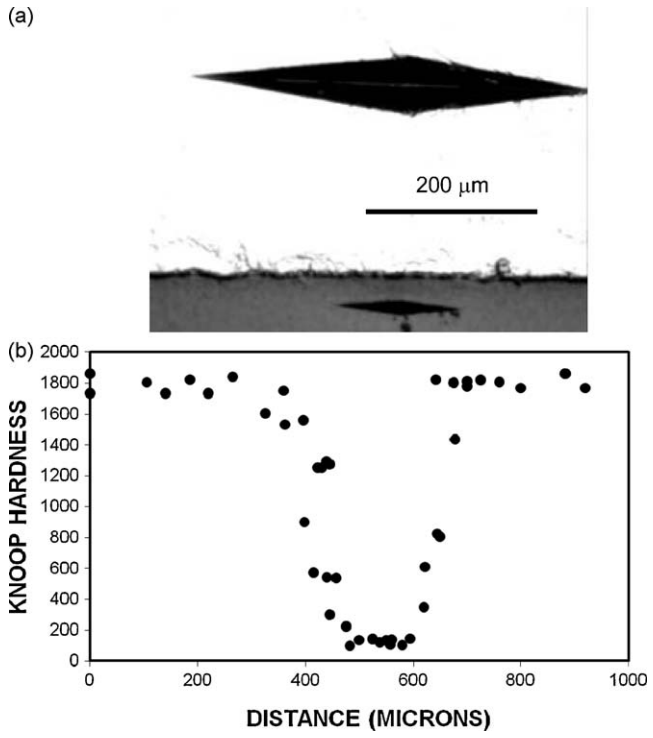

Fig. 8. (a) Optical micrograph of Knoop indentations at the joint layer (upper one) and at the Si_3N_4 piece (lower one). (b) Plot of the Knoop hardness through the joint interlayer.

ted versus the distance across the joint. Knoop hardness of 1800 ± 100 HK was measured for Si_3N_4 and of 130 ± 40 HK for the joint. Multiple profiles accessed across the joint confirmed the reproducibility of the hardness measurements. Indentations performed in the Si_3N_4/joint interface did not create cracks indicating a strong bond.

4. Conclusions

Robust self-joining of St. Gobain Si_3N_4 (NT-154) using a ductile Cu–Al–Si–Ti active braze was demonstrated. A reaction zone (~2.5–3.5 μm thick) of an approximate composition (in atom%) 63Ti–25Si–9Cu–3N developed at the interface after 30 min brazing at 1317 K. There was no interfacial excess of Y (from Y_2O_3 which is added as a sintering aid to NT-154) and the Si_3N_4/braze interfaces were enriched in Ti and Si. TEM observations showed that the Si_3N_4 had a morphology consisting of large grains (micron size), but the reaction layer microstructure had finer grains (in the range of 20–50 nm). The analysis indicated that the reaction layer is rich in the Ti_5Si_3 phase, which is in good agreement with the atomic composition ratio, compositional maps, and thermodynamical calculations. It seems also plausible that AlN is formed at the Si_3N_4–reaction layer interface.

The room temperature compressive shear strengths of the Si_3N_4/Cu-ABA/Si_3N_4 and Inconel/Cu-ABA/Inconel joints were 140 ± 49 MPa and 207 ± 12 MPa, respectively. High-temperature compressive shear tests yielded the strength values of the Si_3N_4/Si_3N_4 joints at 1023 K and 1073 K of 45 ± 10 MPa and 35 ± 5 MPa, respectively, and the strength of Inconel/Inconel joints at 1023 K and 1073 K as 110 ± 10 MPa and 78 ± 5 MPa, respectively. These initial results are promising as they suggest that even at 260 K above a temperature equal to the 2/3rd of the braze solidus, the Si_3N_4/Si_3N_4 joints had high shear strength.

Acknowledgements

Rajiv Asthana and Julian Martinez-Fernandez acknowledge the support received from the NASA Glenn Research Center. Technical assistance received from Ron Phillips in mechanical testing of joints is also thankfully acknowledged. TEM was performed at CITIUS (University of Sevilla).

References

1. Suganuma K, Miyamoto Y, Koizumi M. Joining of ceramics and metals. *Ann Rev Mater Sci* 1988;**18**:47–73.
2. Peteves SD, Ceccone G, Paulasto M, Stamos V, Yvon P. Joining silicon nitride to itself and to metals. *JOM* 1996;(January):48–53.
3. Loehman RE, Tomsia AP, Pask JA, Johnson SM. Bonding mechanisms in silicon nitride brazing. *J Am Ceram Soc* 1990;**73**(3):552–8.
4. Tomsia AP, Pask JA, Loehman RE. Joining nitride ceramics. *Ceram Eng Sci Proc* 1989;**10**(11–12):1631–54.
5. Hadian AM, Drew RAL. Strength and microstructure of silicon nitride ceramics brazed with Ni–Cr–Si alloys. *J Am Ceram Soc* 1996;**79**(3):659–65.
6. Gopal M, Sixta M, De Jonghe L, Thomas G. Seamless joining of silicon nitride ceramics. *J Am Ceram Soc* 2001;**84**(4):708–12.
7. Paulasto M, Ceccone G, Peteves SD. Joining of silicon nitride with V-active filler metals. In: Eustathopoulos N, Sobczak N, editors. *Proc. Int. Conf. High-Temperature Capillarity*. 1997. p. 290–8.
8. Zhuravlev VS, Prokopenko AA, Kostyuk BD, Gab II, Naidich YV. Joining of Si_3N_4 with Ti-active Cu–Ga and Cu–Sn filler alloys. In: Eustathopoulos N, Sobczak N, editors. *Proc. Int. Conf. High-Temperature Capillarity*. 1997. p. 299–305.

9. Jacquemin J-P, Juve D, Treheux D, Miranzo P, Osendi MI. Joining of Si_3N_4 using Al and Ni interlayers. In: Bellosi A, Kosmac T, Tomsia AP, editors. *Interfacial Science in Ceramic Joining*. Boston: Kluwer Academic Publication; 1998. p. 135–42.
10. Svec PA, Pulc V, Gondar E. Joining of silicon nitride ceramics to Ti alloy with an interlayer. In: Bellosi A, Kosmac T, Tomsia AP, editors. *Interfacial Science in Ceramic Joining*. Boston: Kluwer Academic Publication; 1998. p. 341–8.
11. Blugan G, Janczak-Rusch J, Kuebler J. Properties and fractography of Si_3N_4/TiN ceramic joined to steel with active single layer and double layer braze filler alloys. *Acta Mater* 2004;**52**:4579–88.
12. Brochu M, Pugh MD, Drew RAL. Joining silicon nitride ceramic using a composite powder as active brazing alloy. *Mater Sci Eng* 2004;**A374**:34–42.
13. Liu G, Zou G, Wu A, Zhang D. Improvement of the Si_3N_4 brazed joints with intermetallics. *Mater Sci Eng* 2006;**A415**:213–8.
14. Zhang J, Guo YL, Naka M, Zhou Y. Microstructure and reaction phases in Si_3N_4/Si_3N_4 joint brazed with Cu–Pd–Ti filler alloy. *Ceram Int* 2008;**34**:1159–64.
15. Blugan G, Kuebler J, Bissig V, Janczak-Rusch J. Brazing of silicon nitride ceramic composite to steel using SiC-particle-reinforced active brazing alloy. *Ceram Int* 2007;**33**:1033–9.
16. Brochu M, Pugh MD, Drew RAL. Brazing silicon nitride to an iron-based intermetallic using a copper interlayer. *Ceram Int* 2004;**30**:901–10.
17. Park J-W, Mendez PF, Eager TW. Strain energy distribution in ceramic-to-metal joints. *Acta Mater* 2002;**50**(5):883–99.
18. Chaumat G, Drevet B, Vernier L. Reactive brazing study of silicon nitride to metal joining. *J Eur Ceram Soc* 1997;**17**:1925–7.
19. Lee W-C. Joining of Inconel to silicon nitride. *J Mater Sci* 1997;**32**(1):221–8.
20. Hao HQ, Wang YL, Jin ZH. The effect of interlayer metals on the strength of alumina ceramic and 1Cr18Ni9Ti stainless steel bonding. *J Mater Sci* 1995;**30**(16):4107–11.
21. Xian A-P, Si Z-Y. Interface design for joining pressureless sintered sialon ceramics and 40Cr steel brazing with $Ag_{57}Cu_{38}Ti_5$ filler metal. *J Mater Sci* 1992;**27**:1560.
22. Peteves SD, Paulasto M, Ceccone G, Stamos V. The reactive route to ceramic joining: fabrication, interfacial chemistry and joint properties. *Acta Mater* 1998;**46**(7):2407–14.
23. Asthana R, Singh M. Evaluation of Pd-based brazes to join silicon nitride to copper–clad–molybdenum. *Ceram Int* 2009;**35**(8):3511–5.
24. Peteves SD. Joining nitride ceramics. *Ceram Int* 1996;**22**:527–33.
25. Kuroda K, Kamino T, Imura T. Microstructural and microchemical characterization of intergranular phase in yttria-doped hot-pressed silicon nitride. *J Electron Microsc* 1986;**35**(4):378–83.
26. Eustathopoulos N, Chatain D, Coudurier L. Wetting and interfacial chemistry in liquid metal ceramic systems. *Mater Sci Eng* 1991;**A135**:83–8.
27. Bader E, Zoltai L, Hordler M, Arato P, Singer RF, Kaptay G. Wettability of silicon nitride based ceramics by liquid metals. *Trans JWRI (Jpn)* 2001;**30**:137–42.
28. Zhuravlev V, Prokopenko A, Koval A. Wetting of Si_3N_4 by ternary Ti-containing alloys. *Trans JWRI (Jpn)* 2001;**30**:131–41.